Global Motion of Field-Reversed Configuration Plasma

Kayoko Fujimoto, Eri Tachikawa, Hiroshi Gota, Tsutomu Takahashi, Yasuyuki Nogi

College of Science and Technology, Nihon University, Tokyo

1. Introduction

A field-reversed configuration (FRC) plasma is normally produced by a negative-biased theta-pinch method. It is known that the plasma moves along the symmetric axis of a confinement field. Sometimes it moves away from the confinement region when the straight coil is used. In order to control this inconvenient axial motion, mirror coils are installed at both ends of the straight coil. Then, the FRC is successfully formed and confined by selecting an adequate mirror ratio of the field.

However, it is also known that when the FRC is formed in the mirror field, a violent axial contraction starts from both ends of the coil and moves to the midplane. The plasma expands to the mirror after colliding at the midplane, and then reaches an equilibrium state. Due to these axial behaviors, a quick shift to the equilibrium state is impeded.

The axial contraction is caused by an earlier pinch of the plasma at the mirror than that at the center. Pinch behavior at the formation phase can be simulated using the snowplow model. An example with mirror ratio $R_M = 1.3$ is shown in Fig. 1, where solid lines mean positions of a current sheet at every moment during the pinch. The current sheet at the mirror is always ahead of that at the center. In order that the plasma and magnetic pressure are augmented earlier at the mirror region, a driving force toward the midplane is generated.

At the equilibrium phase, the FRC oscillates around the equilibrium position, which is called the n =0 and 1 mode toroidal motions.[1)] It is explained in Sec.3 that the $n = 1$ mode amplitude reaches

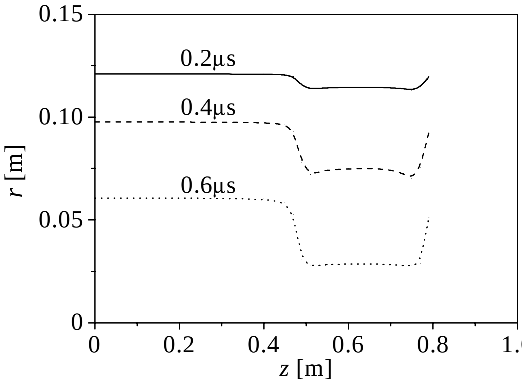

Fig. 1. Time evolution of a current sheet after lift-off from the wall ($r = 0.128$ m) calculated using the snowplow model, where $z = 0$ is the center of the device

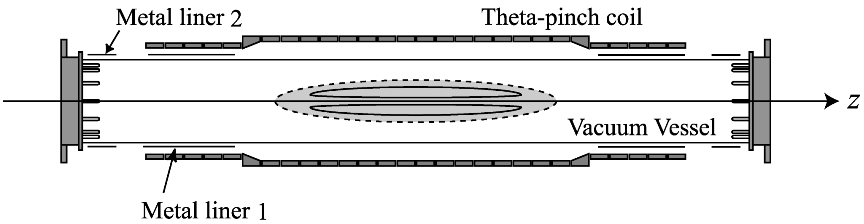

Fig. 2. Schematic of experimental device with two sets of metal liners

about 30% of the separatrix radius in some cases, though the period is very long. Since there is no strong correlation between those motions and the lifetime of the plasma, the motions are not studied in detail. Therefore, the cause of the motion and any adverse influence on the confinement property are not ascertained.

We undertake to minimize the violent axial motion and the toroidal motions, and to study the confinement property without these motions. For this purpose, two sets of metal liners are installed under the mirror coils (metal liner set 1) and outside the coil, (metal liner set 2) as shown in Fig. 2.

Since the penetration time of magnetic field into metal liner set 1 is comparable to a the pinch time of a current sheet in the formation phase, it affects only the formation of the FRC plasma. Therefore, the strength of the magnetic field under the metal liners is weakened during the formation, as shown in Fig. 3, where the mirror ratio with the metal liner is controlled to be lower than that without metal liners. Then, it is expected that the pinch of the current sheet occurs uniformly, as in the straight field, and the violent axial motion is controlled to a low level.

Metal liner set 2 must exert a line-tying effect on the $n=1$ mode motion. For this purpose, lines of magnetic field must penetrate metal liner set 2 until the equilibrium phase is attained. Therefore, the penetration time is set to approximately one period of the $n=1$ mode motion. Metal liner set 2 is set at such a position that the field lines passing through near the separatrix surface cross it.

Improvement of the confinement property with the decrease of the MHD activity in the formation and the equilibrium phase are discussed in this report.

2. Experimental setup

The experimental device NUCTE-III is shown in Fig. 2. It has a 1.5 m length consisting of a 0.9 m center with a 0.34 m bore and 0.3 m mirror parts with a 0.30 m bore. Two sets of metal liners are installed around the vacuum vessel made of a transparent quartz tube with a 2 m length. Metal liner set 1, with a 0.25 m width and 0.25 m bore, is installed under the mirror

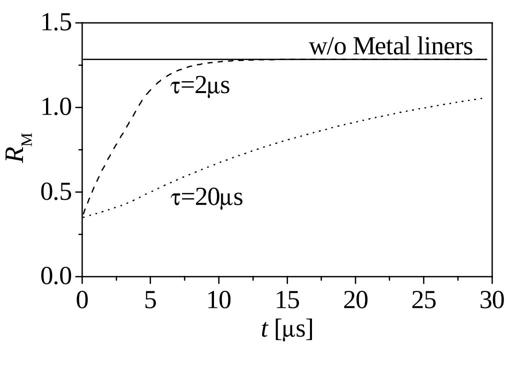

Fig. 3. Time evolution of mirror ratio (field strength under metal liner 1 divided by that at $z=0$) modified by metal liner 1

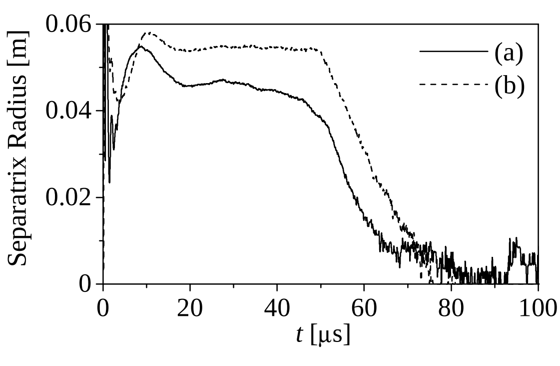

Fig. 4. Separatrix radii at $z=0$ (a) without metal liners and (b) with metal liner 1

coils and metal liner set 2, with a 0.05 m width and a 0.25 m bore, at the ends of the vacuum vessel. All liners are made of a SUS304 steel sheet with 0.3 mm thickness. The penetration time of the magnetic field is $\tau_1 \approx 2\mu s$ for metal liner 1 and $\tau_2 \approx 20\mu s$ for metal liner set 2. Metal liner set 1 has several cuts to control the penetration time. The current flowing in the coil produces a bias field with 0.032 T and a main field with 0.46 T at $t = 3.5\mu$ s and a 110 μ s decay constant without liners. The main field becomes 0.43 T when the metal liners are installed.

The axial behavior of the FRC plasma (n=0 mode) can be determined from the time evolution of a separatrix radius and length, which are obtained by using excluded flux measurement. A line-integrated electron density $\int n_e d\ell$ is measured by a 3.39 μm helium-neon laser interferometer near the center of the device.

An $n = 1$ mode motion is observed by an optical method, in which twenty-eight optical fiber tubes are arrayed near $z = 0$ (axial midplane of the device) along the x -axis and the y -axis to detect the bremsstrahlung for a wavelength of 550 ± 5 nm.[2]

Other constituents of the device and the diagnostic system are described elsewhere.[1,3]

3. Experimental results

The time evolution of the separatrix radius at z =0 is shown in Fig. 4. The radius reaches about 5.5 cm in the first

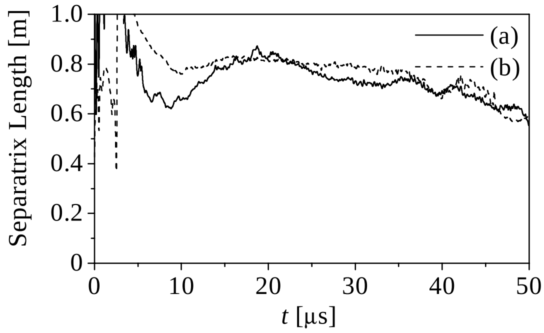

Fig. 5. Time evolution of separatrix lengths (a) without metal liners and (b) with metal liner 1

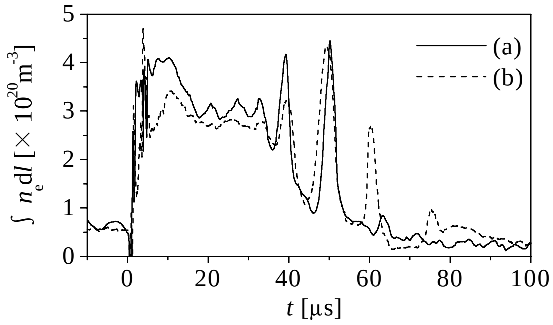

Fig. 6. Line-integrated densities at $z = 0$ (a) without metal liners and (b) with metal liner 1

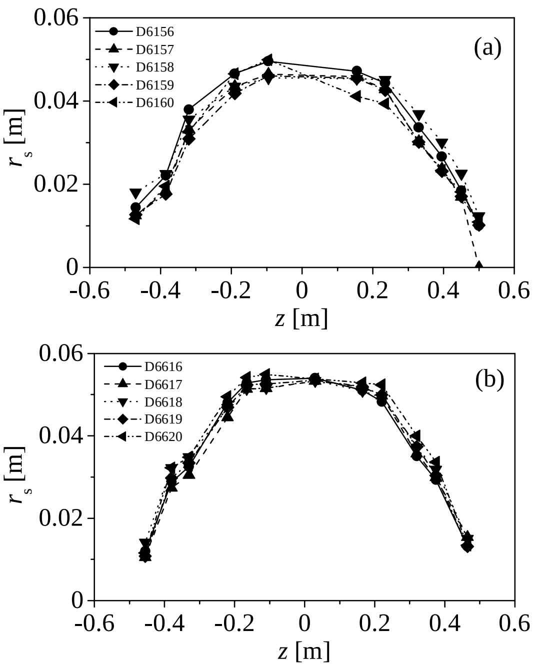

Fig. 7. Separatrix shapes of five FRCs at $t = 20\mu s$ (a) without metal liners and (b) with metal liner 1

$10\,\mu$s and becomes constant after decreasing slightly. The increase of the radius coincides with the decrease of the separatrix length, as shown in Fig. 5. That is, the FRC is temporarily overcompressed by the axial contraction and extends toward the equilibrium form. It is understood that such behavior is mitigated by the use of metal liner set 1. Terminations of both FRCs are caused by the growth of an n =2 mode rotational instability which is manifested as a large-amplitude oscillation in the line-integrated density shown in Fig. 6.

The separatrix shapes of five FRCs produced under the same experimental conditions are superposed in Fig. 7. All plasmas are observed at t =20 μ s. The separatrix shapes of plasma (b) with metal liner set 1 are piled up well compared to plasma (a) without metal liners.

A particle inventory inside the separatrix surface is obtained from $N = \pi r_s^2(0)\ell_s \bar{n}_e$, where $\bar{n}_e = \frac{1}{2r_s(0)}\int n_e d\ell$. The particle confinement time τ_N is derived from a decay constant of the inventory as shown in Fig. 8. They are $\tau_N = 74 \pm 5\mu s$ with metal liner 1 and $\tau_N = 47 \pm 4\mu s$ without metal liners. Since the improvement of τ_N is sometimes observed when the confinement field is weak, the present result must be confirmed by using an FRC with the same field strength as in the

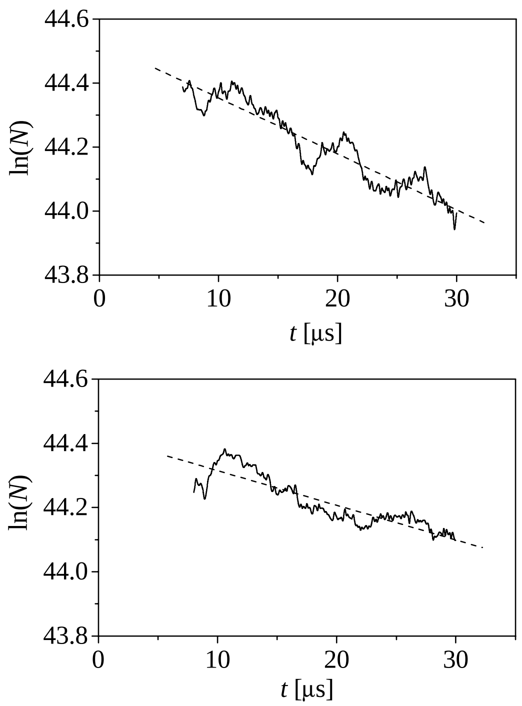

Fig. 8. Time evolution of particle inventories (solid line) and fitting lines (dashed line) (a) without metal liners and (b) with metal liner 1

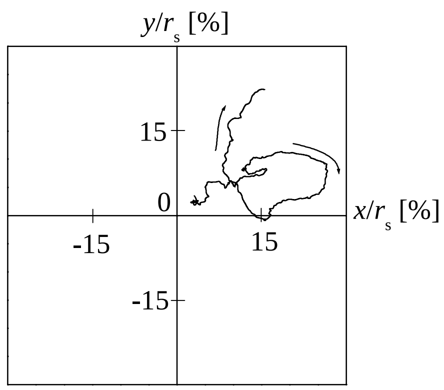

Fig. 9. Trajectory of major axis of the FRC on the $x-y$ plane during $t = 5 \sim 37\mu s$ without metal liners.

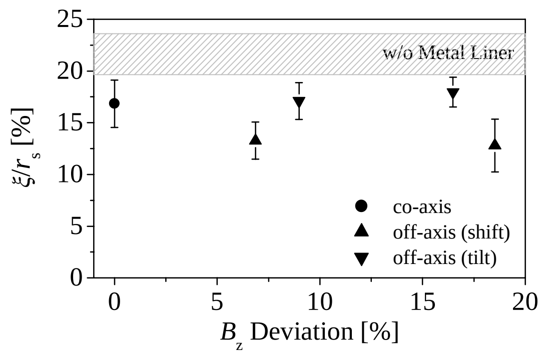

Fig. 10. Amplitude of the $n=1$ mode motion versus installation error of metal liner 1

experiment with metal liner set 1.

The $n=1$ mode motion can be determined from the center coordinates ξ_x and ξ_y of the radiation profiles measured from the optical arrays along the x- and the y-axis. An example of the motion without metal liners is depicted in Fig. 9, where both axes are normalized by the separatrix radius $r_s(t)$ at each time. The FRC plasma produced near the $z-$axis soon moves toward the vacuum vessel. In most cases, the plasma rotates in the same direction as the diamagnetic drift of ions, as shown by the arrows in Fig. 9. The deviation of the FRCs from the $z-$axis is summarized in Fig. 10, where $\xi=\sqrt{\xi_x^2+\xi_y^2}$. The abscissa represents asymmetry rate of the magnetic field on the inner wall of the vacuum vessel when the metal liner is slightly shifted from the original position. For example, asymmetry of 7% arises from a 1.5mm off-axis alignment between the vacuum vessel and the liner. It is controlled to a low level, $\xi/r_s \approx 10 \sim 18\%$, when metal liner set 1 is installed, but is $\xi/r_s \approx 19 \sim 28\%$ without liners. ξ/r_s does not depend on the installation error of metal liner set 1.

The experiment with metal liner set 2 is under way. The result will be reported at the next workshop.

4. Summary

Global motions of FRC plasmas are controlled using a set of metal liners installed under the mirror coils. The first role of the metal liners is to weaken the axial contraction in the mirror field in the formation phase. The second role is to control the axial and radial motions of the FRC in the equilibrium phase.

It was found that the mirror ratio can be adjusted to $R_M=0.8\sim1.0$ in the formation phase in spite of $R_M=1.3$ without metal liners. The plasma length after weaking of the axial contraction becomes about 30% longer. The amplitude of the $n=1$ mode motion is also decreased to almost half that without metal liners. Consequently, highly reproducible FRCs are obtained in the equilibrium phase. Improvement of particle confinement time is achieved when the metal liners are installed.

Further improvement of the confinement property is expected due to a line-tying effect of using another set of metal liners installed outside the mirror coil.

References

1) K. Fujimoto, A. Hoshikawa, S. Ohmura, T. Takahashi, and Y. Nogi, Phys. Plasmas, **9**, 171 (2002).

2) T. Takahashi, T. Asai, Y. Narushima, Y. Ohkuma, and Y. Nogi, Proceedings of 1st General Assembly of Asian Plasma and Fusion Association Joint with 3rd Asia Pacific Plasma Theory Conference, Beijing, 1998, edited by X. T. He (Chinese Physics Society (Chinese Physics

Letters), Beijing, China, 2000), p. 92.
3) Y. Ohkuma, M. Urano, M. Nakamura, Y. Narushima, T. Takahashi, and Y. Nogi, Nucl. Fusion **38**, 1501 (1998).